Single-Molecule Studies

DOI: 10.1002/ange.200602289

# A Simple Nanomixer for Single-Molecule Kinetics Measurements**

*Samuel S. White, Shankar Balasubramanian, David Klenerman,* and Liming Ying**

Single-molecule experiments have enabled the study of subpopulations and multiple reaction pathways by removing the ensemble averaging in bulk experiments.[1] However, to date most single-molecule fluorescence experiments have been performed under equilibrium conditions, which limits the range of measurements for protein and nucleic acid folding or unfolding and precluded the study of weakly bound complexes that would dissociate under equilibrium conditions. One methodology to perform single-molecule studies far from equilibrium is by using a micro- or nanofluidic mixing device.[2,3] Eaton and co-workers coupled a microfabricated laminar-flow mixer to a confocal microscope to examine the folding kinetics of an individual cold shock protein (Csp).[2] Their device offers a time resolution of around 100 ms and can study reactions as long as 10 s. Herein we present a new methodology for studying reaction kinetics at the single-molecule level by incorporating a 100-nm-diameter glass pipette into a confocal optical system to form a quasi-continuous-flow nanomixer, as shown in Figure 1. Our nanomixer offers a slightly better time resolution and approximately the same time-scale as Eaton's system.[2] This new methodology has the added advantages of a reduced background, as measurements are made in free solution, and more importantly simple device fabrication, which should make the method widely applicable.

The nanomixer is based around a nanopipette that we previously developed for the controlled delivery and nanowriting of biomolecules.[4] As almost the entire electric field drop occurs at the tip, when a moderate potential difference is applied across the pipette, biomolecules (in buffer 1) are driven from the tip by a combination of electrophoretic, dielectrophoretic, and electroosmotic forces (see the Supporting Information for a schematic of the basic principle of the device).[4c] Measurements of the diffusion constant by fluorescence correlation spectroscopy near the opening of the pipette tip showed that there was no detectable net flow at a distance 2 μm away from the pipette tip.

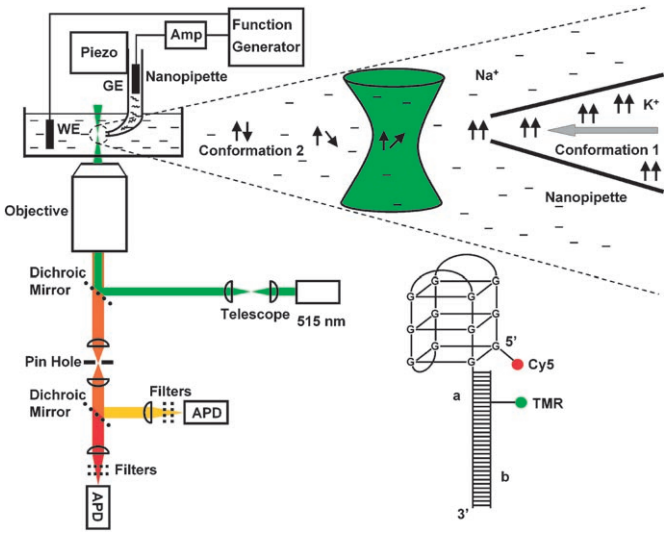


***Figure 1.*** Experimental setup and quadruplex used. Amp = current and voltage amplifier ($\times 10^8$), WE = working electrode, GE = ground electrode.

We approximated the motion of the biomolecules outside the pipette as radial diffusion by using a simple "single-pore" model.[5] The concentration profile $C(r)$ at a radius $r$ away from the pipette opening can be described by Equation (1), in which $C_S$ represents the concentration of the molecule at the pipette tip.[5,6]

$$C(r) = \left(\frac{r_0}{r}\right) C_S \qquad (1)$$

For a disk-shaped pore, such as for the pipettes used in this study, with radius $a$, the radius of the corresponding hemispherical pore $r_0$ can be described by Equation (2).[5]

$$r_0 = \frac{2a}{\pi} \qquad (2)$$

To verify this model the fluorescence of Alexa-647 in Alexa-647-labeled yellow-fluorescent protein (YFP), which is proportional to the YFP concentration, was measured as a function of distance from the pipette tip. The data were fitted to Equation 1 by using the radius of the nanopipette for $a$ (50 nm); the fitted data are shown as the gray line in Figure 2. The "single-pore" model fits the data well, which further supports the assumption that the mixing of biomolecules with the bulk solution (buffer 2) is predominately by diffusion.

As biomolecules diffuse through buffer 2, their conformation changes as a result of the difference in buffer

[*] Dr. S. S. White, Dr. S. Balasubramanian, Dr. D. Klenerman, Dr. L. Ying[+]
Department of Chemistry
University of Cambridge
Lensfield Road, Cambridge CB21EW (UK)
Fax: (+44) 1223-336-362
E-mail: dk10012@cam.ac.uk
ly206@cam.ac.uk

[+] Current Address:
Biological Nanoscience Section
National Heart and Lung Institute
Imperial College London
London SW72AZ (UK)

[**] We thank Joe Piper for the help in diffusion-constant measurements, and Andreas Bruckbauer and Victor Ostanin for constructive discussions about diffusion from the pipette. This work was funded by the Biotechnology and Biological Sciences Research Council, UK.

Supporting information (experimental details, device schematic, derivation of Equation (3), and population assignment) for this article is available on the WWW under http://www.angewandte.org or from the author.

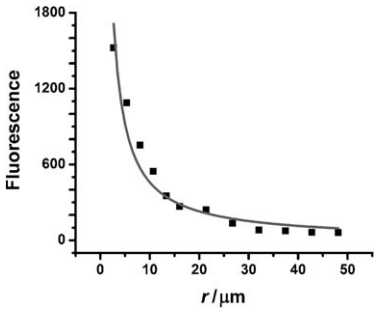


***Figure 2.*** Fluorescence/concentration variation of YFP with distance from the pipette tip. The gray line is a fit of Equation (1) with $r_0 = 0.032$ μm ($a = 50$ nm).

conditions, and this change can be probed by fluorescence spectroscopy. Molecules are probed at different distances $x$ from the pipette tip, and the time $t_{max}$ at which there is maximal probability to observe the molecules is related to $x$ by Equation (3).

$$x^2 = 6\,D\,t_{max} \tag{3}$$

$D$ is the one-dimensional diffusion constant (see the Supporting Information for the derivation, which is based on Einstein's relation for 3D diffusion). This relationship allows kinetic measurements to be made. The dead time of the nanomixer, which limits the time resolution possible, is about 10 ms and depends on how close to the pipette tip it is possible to make measurements without directional flow and the diffusion coefficient of the biomolecule of interest.

We first tested the nanomixer by measuring the dissociation rate constant of an eight-base-pair duplex DNA molecule labeled with a donor and acceptor dye pair. The two complementary strands stay associated inside the pipette, where the sample concentration is well above $K_d$ in 100 mM NaCl. When the duplex DNA is driven out of the pipette, its concentration quickly decreases to well below $K_d$, which results in dissociation of the two strands. A typical fluorescence resonance energy transfer (FRET) decay curve as a function of reaction time is shown in Figure 3. The dissociation rate constant measured by the nanomixer is $2.6 \pm 0.4\ s^{-1}$ in comparison to the value of $1.2 \pm 0.2\ s^{-1}$ observed from

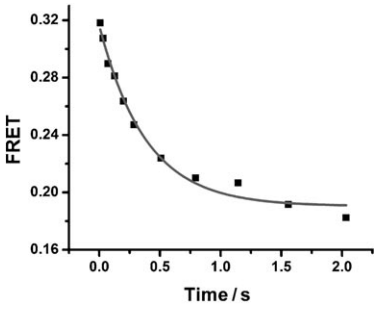


***Figure 3.*** FRET decay as a function of reaction time after a model duplex DNA labeled with Rhodamine green and Alexa-647 at a concentration of 100 nM was quickly diluted by the nanomixer into a buffer (100 mM $Na^+$).

kinetics measurement of the same sequence of duplex DNA by Bayley and co-workers using a protein nanopore.[7] This slightly faster dissociation time is expected, as the DNA we used was labeled with fluorophore at both ends of the duplex, which marginally destabilizes the duplex.

We then applied the nanomixer to study the unfolding kinetics of the human telomeric DNA quadruplex at the single-molecule level. We studied a quadruplex system (Figure 1) that has been previously investigated in detail under equilibrium conditions by single-molecule FRET between a TMR donor and a Cy5 acceptor.[8] In these experiments, the quadruplex was attached to a 35-bp duplex DNA molecule so that there is no change in diffusion coefficient in its different conformations. This situation was confirmed by experiment by using fluorescence correlation spectroscopy (see the Supporting Information). The human intramolecular telomeric G-quadruplex (HITQ) comprises the repeat sequence d(TTAGGG) and has been the subject of considerable study during the past decade because of its links with telomere regulation and cancer.[9] The HITQ can adopt two principal conformations, parallel and antiparallel, which are to a degree dependent on the monovalent cation present and its concentration.[10,11] It is now recognized that in both sodium and potassium buffers, HITQ forms a mixture of parallel and antiparallel quadruplexes but with different ratios,[8,12] although a very recent paper has reported that in potassium solution, HITQ may adopt a hybrid structure with parallel and antiparallel strands.[13]

An equilibrium single-molecule FRET histogram of the HITQ in 1 mM $Na^+$ buffer is shown in the lower panel of Figure 4 (magenta histogram). Two peaks can be clearly seen, one with a center at a transfer efficiency of 0.32 and another near zero. The FRET peak centered near zero is a combination of the unfolded quadruplex (see the Supporting Information) and inactive Cy5.[8] The HITQ in 100 mM $K^+$ buffer is shown in the upper panel of Figure 4 (cyan histogram). This histogram again shows two peaks, but the low FRET peak (**II**) at 0.32 has now shifted to a high FRET peak (**I**) centered at 0.78. Although we cannot unequivocally assign the high and low FRET HITQ structures, one possible scenario is that the structure of the low FRET form (**II**) is a type of antiparallel quadruplex and the high FRET form (**I**) is a mixture of a different type of antiparallel and a parallel quadruplex (see the Supporting Information).[8,12,14] This conclusion is supported by the size of the FRET efficiency for these different structures (see the Supporting Information). Representative FRET histograms measured at different distances/times after diffusion out of the pipette are shown in Figure 4. The kinetics experiments were performed with 100 mM $K^+$ buffer in the nanopipette and 1 mM $Na^+$ buffer in the bath.[15] The high FRET peak rapidly decreases with time and the low FRET form correspondingly increases in magnitude. The kinetics for the conformational change can be obtained by assuming a minimal two-state model [Equation (4)].

$$\text{structure } \mathbf{I} \xrightarrow{k_1} \text{structure } \mathbf{II} \tag{4}$$

The decrease in structure **I** was fitted to a first-order rate equation, and the increase in structure **II** of the HITQ was

  

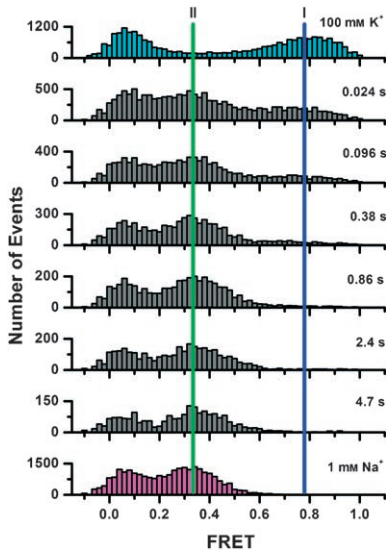


***Figure 4.*** Single-molecule FRET histograms of HITQ during conversion from the high FRET structure to the low FRET structure with 100 mM $K^+$ buffer and 200 nM HITQ in the pipette and 1 mM $Na^+$ buffer in the bath. The cyan FRET histogram is the distribution in 100 mM $K^+$ at equilibrium (top). The magenta FRET histogram is the distribution in 1 mM $Na^+$ at equilibrium (bottom). The green (structure **II**) and blue (structure **I**) solid lines are the centers of the Gaussian function fitted to each population. Data for the FRET histograms were collected for 15 min at different distances from the pipette tip, converted to time by using Equation (3), and represent time after mixing. All experiments were performed at 37 °C.

also fitted to a first-order rate equation (Figure 5). Identical rates were obtained for the decrease in structure **I** and the increase in structure **II** ($k_1 = 5.8 \pm 1.8\ s^{-1}$). The only data available for the unfolding kinetics of the HITQ were obtained at high salt concentration by us[8,16] and Zhao et al.[17] by using the indirect hybridization method. These measurements gave slower unfolding, probably owing to the higher salt concentration used, and the later work was also carried out on a surface-immobilized quadruplex, the kinetics of which may be hindered by the surface. Ha and co-workers also studied surface-immobilized HITQ folding and unfolding; these experiments were carried out under equilibrium conditions in 2 mM $K^+$ solution and gave a unfolding rate of approximately $0.35\ s^{-1}$ at 37 °C.[18] Thus, in view of these differences, our results are consistent with the limited data available for comparison, and importantly our single-molecule measurements allow us to identify any potential intermediate species involved.

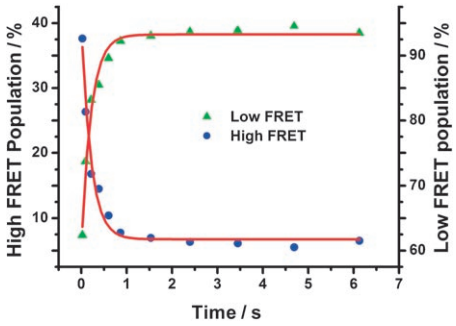


***Figure 5.*** Population variation of the high and low FRET structures with time after mixing. The population of each species was calculated from the area of the Gaussian fits to the FRET histograms in Figure 4. Green triangles represent the low FRET population and blue circles represent the high FRET population. The solid red lines are fits of the data to a first-order rate equation.

In conclusion, a fully functional diffusive nanomixer for single-molecule studies has been developed that allows single-molecule fluorescence studies to be performed under non-equilibrium conditions in free solution without compromising the signal-to-noise ratio. The use of this method has been demonstrated by directly monitoring the subpopulations of the different conformations of a quadruplex during unfolding by using single-molecule FRET to provide complementary kinetic information to previous work.[16–18] Our nanomixer should allow studies of important biological process, such as protein folding, under nonequilibrium conditions in an experimentally simple way.

Received: June 7, 2006
Revised: September 9, 2006
Published online: October 19, 2006

**Keywords:** DNA · FRET (fluorescence resonant energy transfer) · kinetics · single-molecule studies

[1] a) S. Weiss, *Science* **1999**, *283*, 1676–1683; b) X. S. Xie, J. Trautman, *Annu. Rev. Phys. Chem.* **1998**, *49*, 441–480.
[2] E. A. Lipman, B. Schuler, O. Bakajin, W. A. Eaton, *Science* **2003**, *301*, 1233–1235.
[3] a) D. E. Hertzog, X. Michalet, M. Jäger, X. X. Kong, J. G. Santiago, S. Weiss, O. Bakajin, *Anal. Chem.* **2004**, *76*, 7169–7178; b) J. B. Knight, A. Vishwanath, J. P. Brody, R. H. Austin, *Phys. Rev. Lett.* **1998**, *80*, 3863–3866; c) E. Kauffmann, N. C. Darnton, R. H. Austin, C. Batt, K. Gerwert, *Proc. Natl. Acad. Sci. USA* **2001**, *98*, 6646–6649.
[4] a) L. M. Ying, A. Bruckbauer, A. M. Rothery, Y. E. Korchev, D. Klenerman, *Anal. Chem.* **2002**, *74*, 1380–1385; b) A. Bruckbauer, L. M. Ying, A. M. Rothery, D. J. Zhou, A. I. Shevchuk, C. Abell, Y. E. Korchev, D. Klenerman, *J. Am. Chem. Soc.* **2002**, *124*, 8810–8811; c) L. M. Ying, S. S. White, A. Bruckbauer, L. Meadows, Y. E. Korchev, D. Klenerman, *Biophys. J.* **2004**, *86*, 1018–1027; d) K. T. Rodolfa, A. Bruckbauer, D. J. Zhou, Y. E. Korchev, D. Klenerman, *Angew. Chem.* **2005**, *117*, 7014–7019; *Angew. Chem. Int. Ed.* **2005**, *44*, 6854–6859.
[5] A. Kueng, C. Kranz, A. Lugstein, E. Bertagnolli, B. Mizaikoff, *Angew. Chem.* **2005**, *117*, 3485–3488; *Angew. Chem. Int. Ed.* **2005**, *44*, 3419–3422.
[6] E. R. Scott, H. S. White, J. B. Phipps, *Anal. Chem.* **1993**, *65*, 1537–1545.
[7] S. Howorka, L. Movileanu, O. Braha, H. Bayley, *Proc. Natl. Acad. Sci. USA* **2001**, *98*, 12996–13001.
[8] L. M. Ying, J. J. Green, H. T. Li, D. Klenerman, S. Balasubramanian, *Proc. Natl. Acad. Sci. USA* **2003**, *100*, 14629–14634.
[9] S. Neidle, G. Parkinson, *Nat. Rev. Drug Discovery* **2002**, *1*, 383–393.
[10] Y. Wang, D. J. Patel, *Structure* **1993**, *1*, 263–282.
[11] G. N. Parkinson, M. P. H. Lee, S. Neidle, *Nature* **2002**, *417*, 876–880.
[12] a) Y. J. He, R. D. Neumann, I. G. Panyutin, *Nucleic Acids Res.* **2004**, *32*, 18, 5359–5367; b) I. Ourliac-Garnier, M. A. Elizondo-Riojas, S. Redon, N. P. Farrell, S. Bombard, *Biochemistry* **2005**,

  

*44*, 10620 – 10634; c) J. Li, J. J. Correia, L. Wang, J. O. Trent, J. B. Chaires, *Nucleic Acids Res.* **2005**, *33*, 4649 – 4659.
[13] A. Ambrus, D. Chen, J. Dai, T. Bialis, R. A. Jones, D. Yang, *Nucleic Acids Res.* **2006**, *34*, 9, 2723 – 2735.
[14] A. Siddiqui-Jain, C. L. Grand, D. J. Bearss, L. H. Hurley, *Proc. Natl. Acad. Sci. USA* **2002**, *99*, 11593 – 11598.
[15] Under these conditions, the kinetics was sufficiently fast for our instrument. It was too slow at higher sodium concentrations.
[16] J. J. Green, L. M. Ying, D. Klenerman, S. Balasubramanian, *J. Am. Chem. Soc.* **2003**, *125*, 3763 – 3767.
[17] Y. Zhao, Z. Y. Kan, Z. X. Zeng, Y. H. Hao, H. Chen, Z. Tan, *J. Am. Chem. Soc.* **2004**, *126*, 13255 – 13264.
[18] J. Y. Lee, B. Okumus, D. S. Kim, T. Ha, *Proc. Natl. Acad. Sci. USA* **2005**, *102*, 18938 – 18943.

  